



## Sorption of Ni(II) by Fe(II) and EDTA-modified activated carbon derived from pyrophosphoric acid activation

Jing Wang<sup>a,b</sup>, Yan Wang<sup>b,c</sup>, Hai Liu<sup>b</sup>, Jian Zhang<sup>b,\*</sup>, Chenglu Zhang<sup>b</sup>, Jinhe Wang<sup>a</sup>

<sup>a</sup>School of Municipal and Environmental Engineering, Shandong Jianzhu University, Jinan, China, email: wangjing78@126.com (Jing Wang)

<sup>b</sup>Shandong Key Laboratory of Water Pollution Control and Resource Reuse, School of Environmental Science and Engineering, Shandong University, Jinan 250100, China, Tel. +86 531 88363015; Fax: +86 531 88364513; email: angyanyy89@126.com (Y. Wang), hunanliuhai@gmail.com (H. Liu), zhangjian00@sdu.edu.cn (J. Zhang)

<sup>c</sup>College of Earth and Environmental Sciences, Lanzhou University, Lanzhou, Gansu Province 730000, China

Received 18 May 2014; Accepted 30 October 2014

### ABSTRACT

Activated carbon (LSAC) was obtained from lotus stalk by pyrophosphoric acid activation. The LSAC was modified by FeCl<sub>2</sub> and Na<sub>2</sub>EDTA (Fe-EDTA/LSAC) to enhance its ability for Ni(II) sorption from aqueous solutions. The activated carbons were characterized by N<sub>2</sub> adsorption and desorption isotherms, Fourier transform infrared spectroscopy (FTIR), and X-ray diffraction. The sorption of Ni(II) from aqueous solution onto the LSAC and Fe-EDTA/LSAC under various conditions of dosage, contact time, initial solution pH, initial Ni(II) concentration, and ionic strength was investigated to illustrate the mechanism and to quantify the sorption parameters. LSAC and Fe-EDTA/LSAC were mainly microporous with pores almost less than 4 nm. Although the surface area of LSAC (824 m<sup>2</sup>g<sup>-1</sup>) was much higher than that of Fe-EDTA/LSAC (445 m<sup>2</sup>/g), the Ni(II) sorption capacity of Fe-EDTA/LSAC was larger than that of LSAC. The pH and ionic strength studies indicated that the main Ni(II) sorption mechanisms by the carbons were electrostatic attraction and cation exchange. The kinetics and equilibrium data agreed well with the pseudo-second-order kinetics model and Langmuir isotherm model.

*Keywords:* Activated carbon; Modification; Ni(II); Sorption

### 1. Introduction

Nickel (Ni) can become hazardous to organisms if its environmental concentrations exceed a certain level. The severe situation has urged human beings to explore an entire and effective technology to remove these contaminants from wastewater before releasing into the environment [1,2]. Many treatment methods are available for Ni(II) removal, such as membrane fil-

tration, chemical precipitation, ion exchange, and sorption. In these water treatment techniques, sorption is a commonly used method to remove heavy metal ions for its economical efficiency [3–6]. Activated carbon is one of the most widely employed adsorbents due to its well-developed structure, high sorption capacity, and low cost [7–9].

The sorption performance of activated carbons toward heavy metals can be obviously improved by introducing ions, foreign atoms, and organic

\*Corresponding author.

compounds onto the carbon's surface [10–12]. Surface modification of activated carbons is considered as a prospective way to enhance their potentials for specific contaminants, including metals and other inorganic pollutants [13,14]. Ethylenediaminetetraacetic acid (EDTA), with two amine groups and four carboxyl groups, is widely used as a ligand and chelating agent to bind heavy metal ions for forming complexes. EDTA has been employed to modify adsorbents (humic acid, silica gel, graphene oxide, and chitosan [15–17]) for enhancing their sorption capacity toward heavy metals. However, it is not easy to be adsorbed onto carbon material's surface. Some studies have also showed that modification by Fe(II)/Fe(III) can improve the sorption capacity of activated carbon [18–20]. Compared with Fe(III), Fe(II) has less size and can enter the deep pores of porous materials [21]. EDTA has been proved to be easily adsorbed on iron oxide [22,23]. No research has been done on the synthesis of Fe(II) and EDTA-impregnated activated carbon, as well as its sorption capacity of Ni(II). Thus, the activated carbon was firstly impregnated by Fe(II) and then modified by EDTA to introduce more EDTA (amine groups and carboxyl groups) onto the carbon's surface and to promote its Ni(II) sorption capacity.

The present work is to prepare and characterize lotus stalk-based activated carbon functionalized with Fe(II) and EDTA. The sorption potentials of the original and modified activated carbons were investigated for the removal of Ni(II) from aqueous solution under varying dosage, sorption time, initial pH, initial Ni(II) concentration, and ionic strength.

## 2. Materials and methods

### 2.1. Materials

All the chemical reagents used were of analytical grade. The lotus stalk (LS, elemental compositions: C: 48.5%; H: 6.6%; O: 42.3%; N: 2.6%) was obtained from a wetland located in Shandong, China [24]. After harvest, the biomass was washed several times with deionized water, and then dried at 105°C for 24 h. A standard Ni(II) stock solution was prepared by dissolving a certain amount of NiCl<sub>2</sub>(s) in distilled water. Experimental solutions of the desired concentration were obtained by appropriate dilution of the stock solution.

### 2.2. Preparation of activated carbons

Preparation of LSAC: Five grams of dried LS (0.45–1 mm) was fully mixed in H<sub>4</sub>P<sub>2</sub>O<sub>7</sub> solution (45 wt.%) at a ratio of 2/1 (g H<sub>4</sub>P<sub>2</sub>O<sub>7</sub> g<sup>-1</sup> LS). After

impregnation at room temperature for 12 h, the sample was heated in a muffle furnace up to the desired temperature of 450°C and maintained for 1 h. After cooling to room temperature, the activated carbon was thoroughly washed with distilled water until the filtrate attained a constant pH. Finally, the carbon was dried for 12 h at 105°C and sieved to a particle size of 100/140 mesh with standard sieves (Model Φ 200).

Preparation of Fe/LSAC and EDTA/LSAC: about 3 g of LSAC was impregnated into 300 mL ferrous chloride solution (50 mmol L<sup>-1</sup>) or EDTA (50 mmol L<sup>-1</sup>) and shaken at room temperature for 24 h. After vacuum filtration, they were thoroughly washed with distilled water to eliminate the non-adsorbed Fe<sup>2+</sup> and Cl<sup>-</sup> or EDTA. Then, they were dried at 60°C for 6 h and then 105°C for 6 h.

Preparation of Fe-EDTA/LSAC: about 3 g of Fe-LSAC was added to 300 mL EDTA solution (50 mmol L<sup>-1</sup>). Prior to filtration, the mixture was stirred at room temperature for 24 h. It was then washed with distilled water to remove free EDTA, followed by drying at 105°C for 10 h.

### 2.3. Characterizations of LSAC and Fe-EDTA/LSAC

Surface area ( $S_{\text{BET}}$ ) and pore size distribution of LSAC and Fe-EDTA/LSAC were determined by N<sub>2</sub> adsorption and desorption at 77 K with a surface area analyzer (Quantachrome Corporation, USA). The  $S_{\text{BET}}$  was determined using the Brunauer–Emmett–Teller (BET) method and the pore size distribution was obtained by the Density Functional Theory (DFT) method. Total pore volume ( $V_{\text{tot}}$ ) was determined at  $P/P_0 = 0.95$ . External surface area ( $S_{\text{ext}}$ ) and micropore volume ( $V_{\text{mic}}$ ) were calculated using the t-plot method. Average pore diameter ( $D_p$ ) was determined from the relation:  $D_p = 4V_{\text{tot}}/S_{\text{BET}}$ . The surface chemical functional groups of the two carbon samples were also measured with Fourier transform infrared spectroscopy (Fourier-380FTIR, USA). The infrared spectra were recorded between wave numbers of 400–4,000 cm<sup>-1</sup>.

### 2.4. Sorption studies

The Ni(II) sorption kinetics studies were performed by mixing 0.36 g of LSAC and Fe-EDTA/LSAC with 1,000 mL Ni(II) solution (15 mg L<sup>-1</sup>). Then the solution was sampled (20 mL) at each set time ranging from 0 to 12 h, followed by filtrating with a 0.45 μm membrane filter. The Ni(II) concentration in the samples was determined by a UV-vis spectrophotometer (UV-754, Shanghai) at a wavelength of 530 nm [25]. The amount of Ni(II) adsorbed at different times

( $Q_t$ , mg/g) was calculated by the equation:  $Q_t = (C_0 - C_t)V/W$ , where  $C_0$  and  $C_t$  are the initial Ni(II) concentration and the Ni(II) concentration at time  $t$  (mg L<sup>-1</sup>);  $V$  is the solution volume (L); and  $W$  is the mass of adsorbent (g).

For batch equilibrium experiments, a series of certain amounts of the activated carbon were added to Ni(II) solution (50 mL). These experiments were aimed to study the effects of various operating parameters such as dosage, initial Ni(II) concentration, solution pH, and ionic strength on Ni(II) sorption onto LSAC and Fe-EDTA/LSAC. The suspensions were shaken at 90 rpm and  $20 \pm 2^\circ\text{C}$  for 48 h, then the solutions were filtrated before analyzing Ni(II) concentrations. All experiments were performed in duplicates. The sorption amount ( $Q_e$ , mg g<sup>-1</sup>) and removal of Ni(II) at equilibrium were calculated by the equations:  $Q_e(\text{mg/g}) = (C_0 - C_e)V/W$ , removal % =  $(C_0 - C_e) \times 100/C_0$ , where  $C_0$  and  $C_e$  are the initial and equilibrium concentrations of Ni(II) (mg L<sup>-1</sup>);  $V$  is the solution volume (L); and  $W$  is the mass of adsorbent used (g).

### 3. Results and discussion

#### 3.1. Textural characterizations of LSAC and Fe-EDTA/LSAC

The main textural characteristics of the samples are shown in Fig. 1. The N<sub>2</sub> adsorption and desorption isotherms of the two carbons showed a very narrow hysteresis loop, suggesting the characteristics of microporous materials. It is clear that the pore diameter range of LSAC and Fe-EDTA/LSAC was limited within 4 nm from their pore size distributions (Fig. 1). LSAC displayed the higher  $S_{\text{BET}}$  and  $V_{\text{tot}}$  than

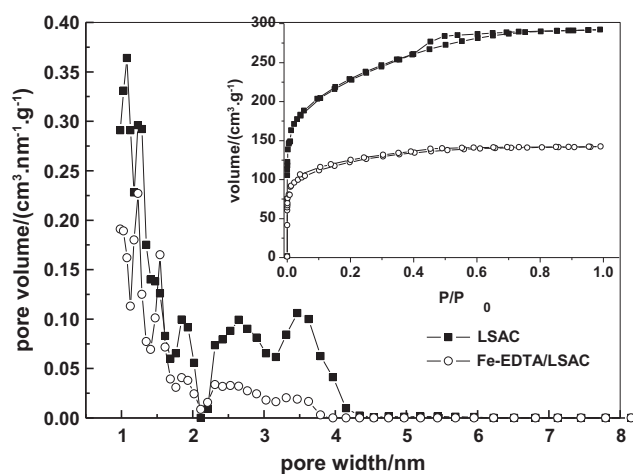


Fig. 1. Pore size distributions and N<sub>2</sub> adsorption/desorption isotherms (inset) of LSAC and Fe-EDTA/LSAC.

Fe-EDTA/LSAC. After modification,  $S_{\text{BET}}$ ,  $S_{\text{mic}}$ , and  $V_{\text{tot}}$  of Fe-EDTA/LSAC obviously decreased from 824 m<sup>2</sup>g<sup>-1</sup>, 759 m<sup>2</sup>g<sup>-1</sup>, and 0.409 cm<sup>3</sup>g<sup>-1</sup> to 445 m<sup>2</sup>g<sup>-1</sup>, 422 m<sup>2</sup>g<sup>-1</sup>, and 0.198 cm<sup>3</sup>g<sup>-1</sup>, respectively.

The X-ray diffraction (XRD) patterns of LSAC were similar and no obvious peaks were observed for Fe-LSAC and Fe-EDTA/LSAC, indicating that Fe was randomly distributed on LSAC's surface (images are not shown here).

#### 3.2. Surface chemistry of LSAC and Fe-EDTA/LSAC

The different surface functional groups of the carbons were identified by Fourier transforms infrared spectroscopy (FTIR). As shown in Fig. 2, the FTIR spectra of LSAC and Fe-EDTA/LSAC displayed intensive bonds at 3,448, 1,633, and 1,124–1,070 cm<sup>-1</sup>, which could be ascribed to stretching ( $\nu$ ) vibrations of O–H, C=O, and C–O, corresponding to the presence of –OH (hydroxyl), C=O (carbonyl), and –COOH (carboxyl) functional groups [26,27]. The peaks at 1,559–1,415 cm<sup>-1</sup> in the spectra of the three carbons were possibly assigned to O–H bending vibrations [28]. From the spectra, it can be seen that there were some more oxygen-containing functional groups on Fe-EDTA/LSAC according to its lower transmittance bands (at 3,448, 1,633, 1,559, and 1,415 cm<sup>-1</sup>) than LSAC.

#### 3.3. Effect of dosage of LSAC or Fe-EDTA/LSAC on Ni(II) sorption

The effect of dosage on the removal of Ni(II) by LSAC and Fe-EDTA/LSAC was examined within

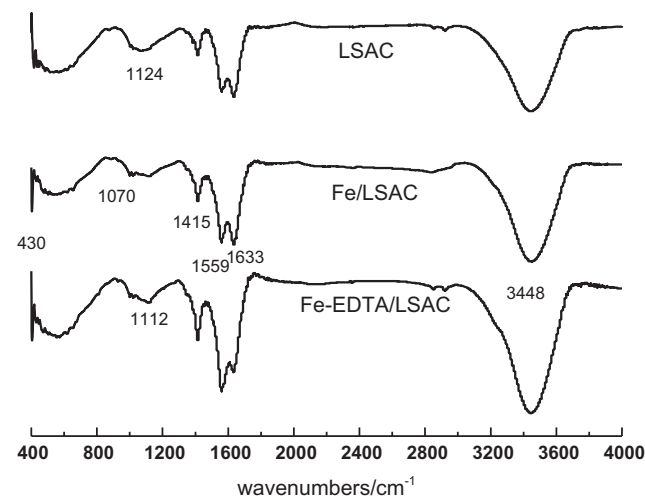


Fig. 2. FTIR spectra of LSAC, Fe/LSAC, and Fe-EDTA/LSAC.

carbon dose range of 0.24–0.40 g L<sup>-1</sup> at an initial Ni(II) concentration of 15 mg L<sup>-1</sup> at 20 ± 2°C for 16 h (Fig. 3). This experiment was carried out to choose a suitable dosage for studying the different sorption capacities of the carbons. The Ni(II) removal increased with the increase in dosage. When the carbon dosage was 0.36 g L<sup>-1</sup>, the removal of Ni(II) by LSAC and Fe-EDTA/LSAC attained nearly 83 and 93%, indicating the suitable dosage for later studies.

### 3.4. Ni(II) sorption kinetics

As shown in Fig. 4, Ni(II) sorption rate onto the carbons was quite rapid in the first 30 min and then gradually slowed down. Equilibrium was attained within about 9 h. The sorption capacity of Fe-EDTA/LSAC (44.8 mg g<sup>-1</sup>) is much higher than that of LSAC (35.2 mg g<sup>-1</sup>).

Sorption kinetics study is essential to understand the capacity of adsorbent and the sorption mechanism [29]. A kinetic investigation was conducted using two kinetic models: (1) Pseudo-first-order model:  $\ln(Q_e - Q_t) = \ln Q_e - K_1 t$ , where  $K_1$  is the rate constant of the pseudo-first-order (min<sup>-1</sup>); (2) Pseudo-second-order model:  $t/Q_t = 1/K_2 Q_e^2 + t/Q_e$ , where  $K_2$  is the equilibrium rate constant of pseudo-second-order (g(mg min)<sup>-1</sup>).

The values of the kinetic parameters as well as the correlation coefficients ( $R^2$ ) for Ni(II) sorption are listed in Table 1. The  $R^2$  obtained from pseudo-first-order model fitting for Ni(II) adsorption onto the two activated carbons were relatively high (0.9999), and the equilibrium adsorption capacities ( $Q_e(\text{cal})$ ) calculated

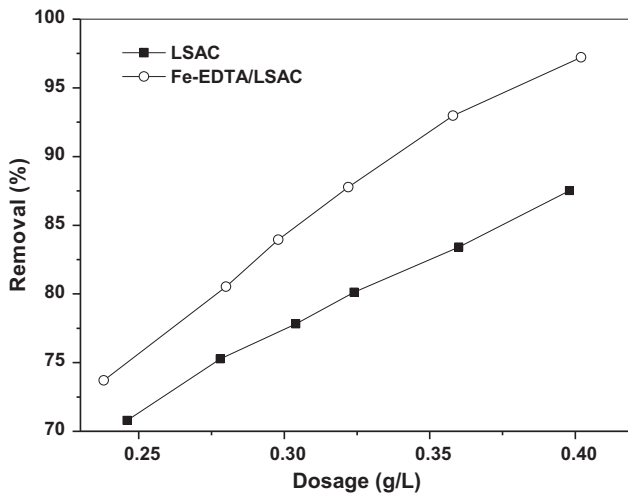


Fig. 3. The effect of dosage of LSAC or Fe-EDTA/LSAC on the removal of Ni(II).

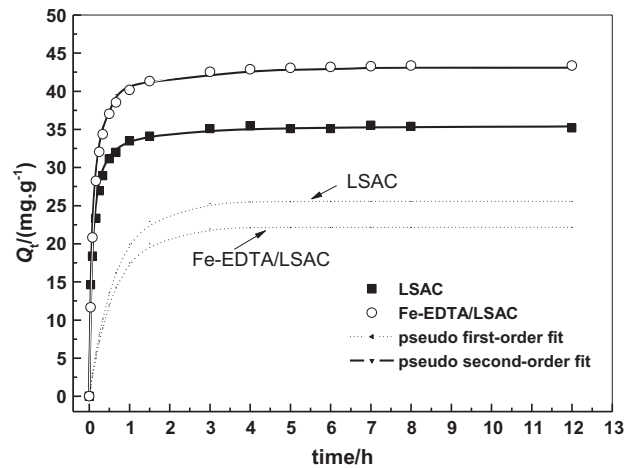


Fig. 4. The effect of contact time on Ni(II) sorption.

from the pseudo-second-order kinetic model were agreed well with the experimental values ( $Q_e(\text{exp})$ ) as well (Table 1). Furthermore, the Ni(II) sorption kinetics for the two carbons were nonlinear tested (Fig. 4). It was shown that the pseudo-second-order kinetic model correlated the kinetic data better than the pseudo-first-order kinetic model, since the line corresponding to the model is closer to the experimental points than that of the pseudo-second-order model. The pseudo-second-order model presumes that the sorption rate is controlled by chemical sorption. For both adsorbents, the ideal fit of this model implied that chemisorption was an important mechanism in sorption, which was consistent with the electrostatic interaction and chemical-bonding mechanism proposed by the following discussion.

### 3.5. Ni(II) sorption isotherms

Langmuir isotherm model is usually chosen for the estimation of the maximum sorption capacity corresponding to complete monolayer coverage on the adsorbent surface. Freundlich isotherm model is based on sorption on heterogeneous surface and active sites with different energies. Equilibrium data (Fig. 5) were analyzed by the Langmuir ( $Q_e = Q_m K_L C_e / (1 + K_L C_e)$ ) and Freundlich ( $Q_e = K_F C_e^{1/n}$ ) isotherm models, where  $Q_m$  (mg g<sup>-1</sup>) is the maximum sorption capacity;  $K_L$  (L mg<sup>-1</sup>) represents the Langmuir constant; and  $K_F$  ((mg g<sup>-1</sup>) (L<sup>1/n</sup> mg<sup>-1/n</sup>)) and  $1/n$  represent the Freundlich constant referring to sorption capacity and intensity, respectively.

The isotherm parameters of Ni(II) onto LSAC and Fe-EDTA/LSAC are shown in Table 2. The values of correlation coefficient ( $R^2$ ) derived from Langmuir

Table 1  
Kinetic parameters for the sorption of Ni(II) onto LSAC and Fe-EDTA/LSAC

Samples	$Q_{e,exp}/(\text{mg g}^{-1})$	Pseudo-first-order			Pseudo-second-order		
		$K_1/\text{h}^{-1}$	$Q_{e,cal}/(\text{mg g}^{-1})$	$R^2$	$K_2/(\text{mg}^{1-n}\text{L}^n\text{g}^{-1})$	$Q_{e,cal}/(\text{mg g}^{-1})$	$R^2$
LSAC	35.2	1.517	25.6	0.8096	0.439	35.6	0.9999
Fe-EDTA/LSAC	44.8	1.557	22.2	0.7909	0.247	43.8	0.9999

Notes: LSAC: lotus stalk-based activated carbon.

Fe-EDTA/LSAC: Fe(II) and EDTA-modified lotus stalk-based activated carbon.

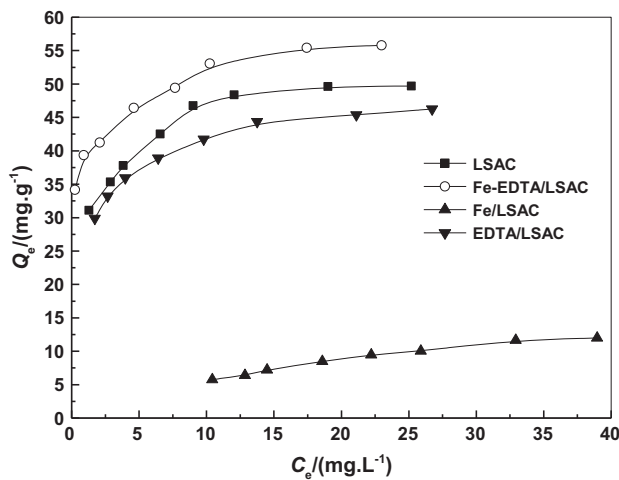


Fig. 5. Sorption isotherms of Ni(II) on the carbons.

model were much larger ( $>0.9970$ ) than those derived from Freundlich model, which indicated that the equilibrium data were simulated better by Langmuir model than by Freundlich model. Langmuir model was quite successful in predicting the experimental saturation capacities, indicating monolayer coverage due to the strong interactions between the carbons' surface and Ni(II). The maximum sorption capacities ( $Q_m$ ) of Fe-EDTA/LSAC were much larger than that

of LSAC. This phenomenon can be attributed to the different surface chemistry of the carbons. The  $n$  values expressed the sorption performance quality and were larger than 1, indicating the preferential sorption.

Equilibrium sorption capacity of Ni(II) on the carbons was ordered as follows: Fe-EDTA/LSAC  $>$  LSAC  $>$  EDTA/LSAC  $>$  Fe/LSAC. These results indicated that the Fe(II)-EDTA-modified method could improve the removal of Ni(II). The Fe/LSAC showed much lower Ni(II) sorption than LSAC, which was due to the occupation of Fe(II) on the sorption sites of LSAC [30]. The EDTA/LSAC presented slightly lower Ni(II) sorption than LSAC, suggesting that EDTA could not be attached effectively on LSAC's surface. A comparison of the maximum Ni(II) sorption capacities of the carbons with other adsorbents is shown in Table 3. In general, LSAC and Fe-EDTA/LSAC had larger Ni(II) sorption capacities than other adsorbents, which suggests that the studied carbons were promising adsorbents toward nickel ions.

### 3.6. Effect of initial pH on Ni(II) sorption

Solution pH extremely affects the ionization of surface functional groups and the species of metal ions [36] and will significantly affect the sorption of heavy metals onto the solid adsorbent [26,37]. Batch sorption

Table 2  
The parameters for Langmuir and Freundlich isotherm models of Ni(II) sorption onto LSAC, Fe-EDTA/LSAC, Fe/LSAC, and EDTA/LSAC

Samples	Langmuir			Freundlich		
	$Q_m/(\text{mg g}^{-1})$	$K_L/(\text{L mg}^{-1})$	$R^2$	$K_F/(\text{mg g}^{-1}\text{mg}^{-1/n})$	$n$	$R^2$
LSAC	50.6	0.742	0.9986	29.53	5.59	0.9475
Fe-EDTA/LSAC	57.1	1.483	0.9983	39.58	8.87	0.9835
Fe/LSAC	21.0	0.036	0.9902	1.49	1.72	0.9859
EDTA/LSAC	48.1	0.889	0.9999	29.15	6.48	0.9317

Notes: LSAC: lotus stalk-based activated carbon.

Fe-EDTA/LSAC: Fe(II) and EDTA-modified lotus stalk-based activated carbon.

Table 3

Comparison of maximum Ni(II) sorption capacity on various adsorbents reported in literature

Adsorbent	$Q_{\max}$ (mg g <sup>-1</sup> )	Reference
Almond husk-activated carbon	30.7	[7]
Apricot stone-activated carbon	27.21	[8]
Ficus carica-activated carbon	18.78	[9]
Apricot-activated carbon	37.59	[31]
<i>Parthenium hysterophorus</i> L.-activated carbon	17.24	[32]
Olive stone	3.63	[33]
Scrap tire	21.28	[34]
Multiwall carbon nanotube	9.18	[35]

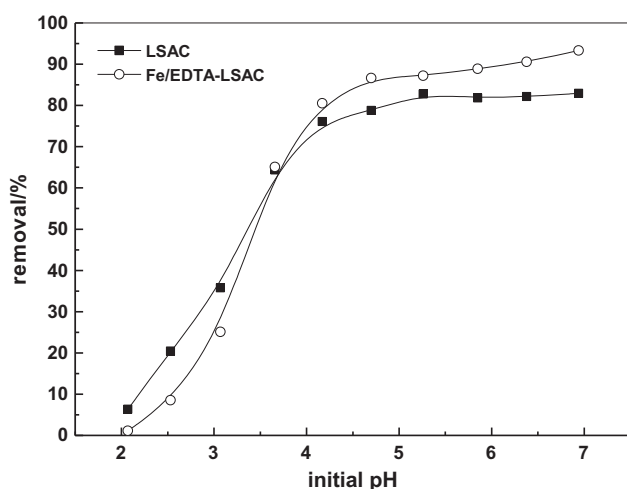


Fig. 6. The effect of pH on Ni(II) sorption.

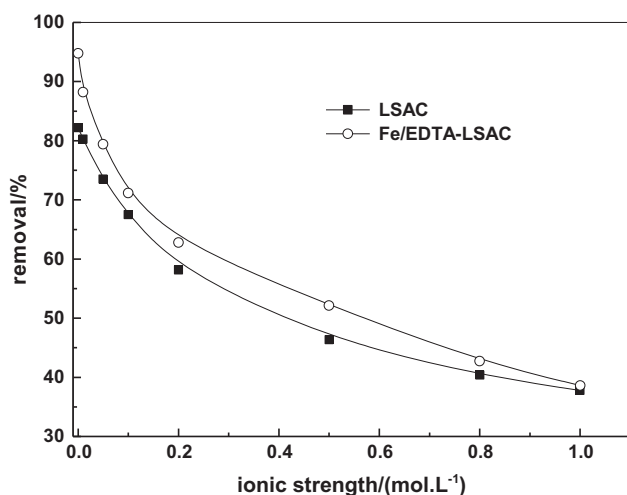


Fig. 7. The effect of ionic strength on Ni(II) sorption.

experiments were carried out to evaluate the effect of pH on Ni(II) sorption. The removal of Ni(II) by the carbons rose dramatically with the increase in initial pH from 2 to 4 (Fig. 6). In this pH range, the Ni(II) removal by LSAC was higher than that by Fe-EDTA/LSAC. At low pH, the H<sup>+</sup> in solution would complete the sorption sites with Ni(II), and the surface of the carbon would be protonized, resulting in the higher electrostatic repulsion between the surface and the Ni(II) cations. Therefore, at low pH, the Ni(II) was rejected to contact the introduced O/N-containing groups on Fe-EDTA/LSAC, leading its sorption lower than LSAC. With the rise in pH, competition between H<sup>+</sup> and Ni<sup>2+</sup> will gradually weaken, and the surface of the carbons will be deprotonized, leading to high Ni(II) sorption through electrostatic attraction [38,39].

### 3.7. Effect of ionic strength on Ni(II) sorption

There are many kinds of interactions between Ni(II) and the carbons that may be responsible for the adsorption. Hence, it is important to assess the effect of ionic strength which is usually used to distinguish between non-specific and specific sorption. If sorption is insensitive to ionic strength, it indicates that adsorbate establishes covalent bonds with the functional groups of adsorbents. The specific sorption was more sensitive to the changes in ionic strength than non-specific sorption [40]. The effect of NaCl concentrations on Ni(II) uptake by the carbons was carried out. As shown in Fig. 7, the removal of Ni(II) decreased dramatically with increasing ionic strength (NaCl), indicating that cation-exchange and electrostatic attraction were important mechanisms responsible for Ni(II) sorption.

## 4. Conclusion

Activated carbon was prepared by pyrophosphoric acid activation and was modified by FeCl<sub>2</sub> and

Na<sub>2</sub>EDTA. The N<sub>2</sub> adsorption and desorption isotherms, FTIR and XRD, were used to characterize the carbons. The results showed that LSAC and Fe–EDTA/LSAC were mainly microporous. The maximum monolayer sorption capacity,  $Q_m$ , for Ni(II) sorption onto Fe–EDTA/LSAC, which was 57.1 mg g<sup>-1</sup>, was larger than the original activated carbon (LSAC) and the LSAC modified by Fe(II) or EDTA only. The kinetics and equilibrium data were fitted well by the pseudo-second-order kinetics model and Langmuir isotherm model. The pH and ionic strength had obvious effects on Ni(II) sorption on the carbons. Several possible adsorption mechanisms were elaborated which include ion-exchange and electrostatic interactions.

### Acknowledgments

This work was supported by the Independent Innovation Foundation of Shandong University (2012JC029), Natural Science Foundation for Distinguished Young Scholars of Shandong Province (JQ201216), National Water Special Project (2012ZX07203-004), and National Natural Science Foundation of China (No. 41305124).

### References

- [1] M. Kasper-Sonnenberg, D. Sugiri, S. Wurzler, U. Ranft, H. Dickel, J. Wittsiepe, J. Hölzer, F. Lemm, G. Eberwein, P. Altmeyer, Prevalence of nickel sensitization and urinary nickel content of children are increased by nickel in ambient air, *Environ. Res.* 111 (2011) 266–273.
- [2] V. Velikova, T. Tsonev, F. Loreto, M. Centritto, Changes in photosynthesis, mesophyll conductance to CO<sub>2</sub>, and isoprenoid emissions in *Populus nigra* plants exposed to excess nickel, *Environ. Pollut.* 159 (2011) 1058–1066.
- [3] H. Javadian, P. Vahedian, M. Toosi, Adsorption characteristics of Ni(II) from aqueous solution and industrial wastewater onto polyaniline/HMS nanocomposite powder, *Appl. Surf. Sci.* 284 (2013) 13–22.
- [4] H. Javadian, F.Z. Sorkhrodi, B.B. Koutenaei, Experimental investigation on enhancing aqueous cadmium removal via nanostructure composite of modified hexagonal type mesoporous silica with polyaniline/polypyrrole nanoparticles, *J. Ind. Eng. Chem.* 20 (2014) 3678–3688.
- [5] H. Javadian, Adsorption performance of suitable nanostructured novel composite adsorbent of poly(N-methylaniline) for removal of heavy metal from aqueous solutions, *J. Ind. Eng. Chem.* 20 (2014) 4344–4352.
- [6] H. Javadian, Application of kinetic, isotherm and thermodynamic models for the adsorption of Co(II) ions on polyaniline/polypyrrole copolymer nanofibers from aqueous solution, *J. Ind. Eng. Chem.* 20 (2014) 4233–4241.
- [7] H. Hasar, Adsorption of nickel(II) from aqueous solution onto activated carbon prepared from almond husk, *J. Hazard. Mater.* 97 (2003) 49–57.
- [8] M. Kobya, E. Demirbas, E. Senturk, M. Ince, Adsorption of heavy metal ions from aqueous solutions by activated carbon prepared from apricot stone, *Bioreour. Technol.* 96 (2005) 1518–1521.
- [9] J. Wang, H. Liu, S. Yang, J. Zhang, C. Zhang, H. Wu, Physicochemical characteristics and sorption capacities of heavy metal ions of activated carbons derived by activation with different alkyl phosphate triesters, *Appl. Surf. Sci.* 316 (2014) 443–450.
- [10] M. Sereych, D. Hulicova-Jurcakova, G.Q. Lu, T.J. Bandosz, Surface functional groups of carbons and the effects of their chemical character, density and accessibility to ions on electrochemical performance, *Carbon* 46 (2008) 1475–1488.
- [11] H. Liu, P. Dai, J. Zhang, C. Zhang, N. Bao, C. Cheng, L. Ren, Preparation and evaluation of activated carbons from lotus stalk with trimethyl phosphate and tributyl phosphate activation for lead removal, *Chem. Eng. J.* 228 (2013) 425–434.
- [12] H. Liu, Q. Gao, P. Dai, J. Zhang, C. Zhang, N. Bao, Preparation and characterization of activated carbon from lotus stalk with guanidine phosphate activation: Sorption of Cd(II), *J. Anal. Appl. Pyrolysis* 102 (2013) 7–15.
- [13] C. Yin, M. Aroua, W. Daud, Review of modifications of activated carbon for enhancing contaminant uptakes from aqueous solutions, *Sep. Purif. Technol.* 52 (2007) 403–415.
- [14] A. Bhatnagar, W. Hogland, M. Marques, M. Sillanpää, An overview of the modification methods of activated carbon for its water treatment applications, *Chem. Eng. J.* 219 (2013) 499–511.
- [15] E. Repo, J.K. Warchoł, A. Bhatnagar, M. Sillanpää, Heavy metals adsorption by novel EDTA-modified chitosan–silica hybrid materials, *J. Colloid Interface Sci.* 358 (2011) 261–267.
- [16] C.J. Madadrang, H.Y. Kim, G. Gao, N. Wang, J. Zhu, H. Feng, M. Goring, M.L. Kasner, S. Hou, Adsorption behavior of EDTA-graphene oxide for Pb(II) removal, *Appl. Mater. Interface* 4 (2012) 1186–1193.
- [17] Z. Wu, Z. Gu, X. Wang, L. Evans, H. Guo, Effects of organic acids on adsorption of lead onto montmorillonite, goethite and humic acid, *Environ. Pollut.* 121 (2003) 469–475.
- [18] H. Liu, B. Qing, X. Ye, Q. Li, K. Lee, Z. Wu, Boron adsorption by composite magnetic particles, *Chem. Eng. J.* 151 (2009) 235–240.
- [19] X.-J. Yang, H.-S. Zhu, L. Yang, X.-L. Long, W.-K. Yuan, A study on the reduction of [Fe(III)-EDTA]–Catalyzed with activated carbon in a fixed-bed, *Environ. Prog. Sustainable Eng.* 32 (2013) 206–212.
- [20] H. Liu, W. Liu, J. Zhang, C. Zhang, L. Ren, Y. Li, Removal of cephalixin from aqueous solutions by original and Cu(II)/Fe(III) impregnated activated carbons developed from lotus stalks kinetics and equilibrium studies, *J. Hazard. Mater.* 185 (2011) 1528–1535.
- [21] W. Liu, J. Zhang, C. Zhang, L. Ren, Preparation and evaluation of activated carbon-based iron-containing adsorbents for enhanced Cr(VI) removal: Mechanism study, *Chem. Eng. J.* 189–190 (2012) 295–302.

- [22] B. Nowack, L. Sigg, Adsorption of EDTA and Metal-EDTA complexes onto Goethite, *J. Colloid. Interface Sci.* 177 (1996) 106–121.
- [23] B. Nowack, J. Lützenkirchen, P. Behra, L. Sigg, Modeling the adsorption of metal-EDTA complexes onto oxides, *Environ. Sci. Technol.* 30 (1996) 2397–2405.
- [24] H. Liu, J. Zhang, N. Bao, C. Cheng, L. Ren, C. Zhang, Textural properties and surface chemistry of lotus stalk-derived activated carbons prepared using different phosphorus oxyacids: Adsorption of trimethoprim, *J. Hazard. Mater.* 235–236 (2012) 367–375.
- [25] J. Zhu, B. Deng, J. Yang, D. Gang, Modifying activated carbon with hybrid ligands for enhancing aqueous mercury removal, *Carbon* 47 (2009) 2014–2025.
- [26] J. Chen, Y. Zhai, H. Chen, C. Li, G. Zeng, D. Pang, P. Lu, Effects of pretreatment on the surface chemistry and pore size properties of nitrogen functionalized and alkylated granular activated carbon, *Appl. Surf. Sci.* 263 (2012) 247–253.
- [27] Z. Jamalzadeh, M. Haghghi, N. Asgari, Synthesis, physicochemical characterizations and catalytic performance of Pd/carbon-zeolite and Pd/carbon-CeO<sub>2</sub> nanocatalysts used for total oxidation of xylene at low temperatures, *Front. Environ. Sci. Eng.* 7 (2013) 365–381.
- [28] A.M. Puziy, O.I. Poddubnaya, A. Martínez-Alonso, F. Suárez-García, J.M.D. Tascón, Surface chemistry of phosphorus-containing carbons of lignocellulosic origin, *Carbon* 43 (2005) 2857–2868.
- [29] J. Lin, L. Wang, Comparison between linear and non-linear forms of pseudo-first-order and pseudo-second-order adsorption kinetic models for the removal of methylene blue by activated carbon, *Front. Environ. Sci. Eng.* 3 (2009) 320–324.
- [30] Z. Wang, E. Nie, J. Li, M. Yang, Y. Zhao, X. Luo, Z. Zheng, Equilibrium and kinetics of adsorption of phosphate onto iron-doped activated carbon, *Environ. Sci. Pollut. R.* 19 (2012) 2908–2917.
- [31] S. Erdoğan, Y. Önal, C. Akmil-Başar, S. Bilmiz-Erdemoglu, Ç. Sarıci-Özdemir, E. Köseoğlu, G. İçduygu, Optimization of nickel adsorption from aqueous solution by using activated carbon prepared from waste apricot by chemical activation, *Appl. Surf. Sci.* 252 (2005) 1324–1331.
- [32] H. Lata, V.K. Garg, R.K. Gupta, Sequestration of nickel from aqueous solution onto activated carbon prepared from *Parthenium hysterophorus* L, *J. Hazard. Mater.* 157 (2008) 503–509.
- [33] N. Fiol, I. Villaescusa, M. Martínez, N. Miralles, J. Poch, J. Serarols, Sorption of Pb(II), Ni(II), Cu(II) and Cd(II) from aqueous solution by olive stone waste, *Sep. Purif. Technol.* 50 (2006) 132–140.
- [34] V.K. Gupta, A. Suhas, S. Nayak, M. Agarwal, I. Chaudhary, Tyagi, Removal of Ni (II) ions from water using scrap tire, *J. Mol. Liq.* 190 (2014) 215–222.
- [35] C. Chen, J. Hu, D. Shao, J. Li, X. Wang, Adsorption behavior of multiwall carbon nanotube/iron oxide magnetic composites for Ni(II) and Sr(II), *J. Hazard. Mater.* 164 (2009) 923–928.
- [36] J. Orfao, A. Silva, J. Pereira, S. Barata, I. Fonseca, P. Faria, M. Pereira, Adsorption of a reactive dye on chemically modified activated carbons—Influence of pH, *J. Colloid. Interface Sci.* 296 (2006) 480–489.
- [37] S. Chen, Q. Yue, B. Gao, X. Xu, Equilibrium and kinetic adsorption study of the adsorptive removal of Cr(VI) using modified wheat residue, *J. Colloid. Interface Sci.* 349 (2010) 256–264.
- [38] M.I. Kandah, J.-L. Meunier, Removal of nickel ions from water by multi-walled carbon nanotubes, *J. Hazard. Mater.* 146 (2007) 283–288.
- [39] L. Huang, Y. Sun, T. Yang, L. Li, Adsorption behavior of Ni (II) on lotus stalks derived active carbon by phosphoric acid activation, *Desalination* 268 (2011) 12–19.
- [40] J. Lützenkirchen, Ionic strength effects on cation sorption to oxides: Macroscopic observations and their significance in microscopic interpretation, *J. Colloid. Interface Sci.* 195 (1997) 149–155.